Chapter 5. RF Systems

M. Champion, W. Chou, J. Griffin, K. Koba, J. MacLachlan, A. Moretti,
M. Popovic, Z. Qian, J. Reid, J. Steimel, D. Wildman

5.1. Introduction

In this section two completely separate Proton Driver rf systems are described. Because of space limitations in the lattice it will not be possible to install and/or operate the two systems concurrently. For Stage 1 operation, a 37 - 53 MHz rf system will be installed. Development for this application of a large aperture (5"), increased voltage modification of an existing Fermilab Booster rf cavity is described in Sec. 5.2.2. As an alternative, efforts have begun on modification of the TRIUMF/SSC style orthogonally biased ferrite rf cavity, cf. Sec. 5.2.3.

For Stage 2 operation the 53 MHz system will be removed, and a lower frequency, harmonic number 18, rf system will be installed. For this system, development of an rf cavity using a new nanocrystalline soft magnetic material, Finemet, is described in Sec. 5.3.2. The lower frequency cavities may use some ferrite tuner components obtained from the removed 53 MHz cavities for tuning during acceleration.

The rf parameters for the two stages are summarized in Table 5.1.

Table 5.1. Summary of RF Parameters

Stage 1 rf parameters (Section 5.2)	Stage 2 rf parameters (Section 5.3)
Harmonic number 126, with 119 occupied buckets.	Harmonic number 18, with all buckets occupied.
Extraction longitudinal emittance, (95%), 0.1 eV-s per bunch.	Extraction longitudinal emittance, (95%), 0.4 -0.5 eV-s per bunch.
Rf frequency range: 37.8 - 53 MHz.	Rf frequency range: 5.4 - 7.6 MHz.
Maximum ring voltage: 1.2 MV.	Maximum ring voltage: 1.4 MV
Average rf power to beam (66.6 ms period) ~ 835 kW	Average rf power to beam (66.6 ms period) ~1.2 MW.
Peak rf power to beam capability ~2 MW.	Peak rf power to beam capability ~ 2.9 MW.
	Extracted bunch length ~ 1 ns rms (neutrino source operation).

Section 5.2, (Stage 1), describes an rf system which is consistent with use of the Proton Driver as an injector for the Main Injector ring in "normal" operation. In this mode the ring will operate from injection energy 400 MeV to extraction energy 12 GeV with intensity ~3×10^{13} protons per cycle. The guide fields will be sinusoidal at 15 Hz, with a 12.5% second harmonic component, phased so as to optimize certain rf voltage and bucket area parameters.

Section, 5.3, (Stage 2), describes an rf system to be used in neutrino source service, but also capable of injecting widely spaced intense bunches into matched Main Injector buckets. In this mode the extraction energy will be 16 GeV with beam intensity 3×10^{13} protons per cycle. Guide field parameters will be similar to those described above.

In each case the rf accelerating voltage, $V\sin\varphi_s$, is defined uniquely by the ring circumference and the rate of rise of the magnetic guide field, dB/dt. The additional rf voltage necessary to obtain the design intensities, longitudinal emittances, and bunch configurations proposed for each of the Proton Driver stages have been elucidated through extensive simulations of rf capture, acceleration, and bunch manipulation prior to extraction, using the code ESME. In each case the effect of installation of space charge compensating inductance (see Section 5.1.1) has been included in the calculations. Also, the higher harmonic effects of frequency variation of the parameters of the introduced inductance have been simulated. Descriptions of these simulations and their results for Stage 1 and Stage 2 acceleration are presented in 5.2.1, 5.2.2, 5.3.1, and 5.3.2. For injection into the Main Injector, the rf voltage and bucket area will be adjusted during acceleration such that extracted bunches will be matched to stationary buckets in the Main Injector. In neutrino source application, the rf voltage will be manipulated prior to extraction so that the extracted bunch length will be ≤ 1 ns rms.

5.1.1 Beam Loading.

With intensity 3×10^{13} protons per cycle, design techniques for compensation of various forms of beam loading must be incorporated. This is especially true in Stage 2, where, at $h = 18$, the charge per bunch will be 1.67×10^{12} protons per bunch ($0.27\ \mu C$). The amplitude and phase of the net rf voltage will be affected by cavity excitation by fundamental and lower harmonic Fourier components of the beam current. These beam loading errors are to be corrected by a global feedback system in which unwanted beam phase motion, detected by broad-band beam pick-ups, will be compensated for by correction signals delivered to each rf station. Global feedback systems are described in 5.2.4, 5.2.6, 5.3.3, and 5.3.5.

Below transition the charges in each bunch interact with the vacuum chamber conducting wall in such a way as to reduce the rf focusing force and bucket area [1]. It has been pointed out, by A. Sessler and V. Vaccaro [2], that this "potential well distortion" may be minimized by the intentional introduction of inductance into the vacuum chamber.

The effect of installed inductance has been studied in the KEK Proton Synchrotron. Because the potential well distortion moves with the charge distribution, the coherent synchrotron dipole phase oscillation frequency is not affected. Predicted changes in incoherent phase oscillation frequency, representing changes in the bucket area, were observed by measurement of the synchrotron quadrupole frequency as a function of beam intensity with fixed rf voltage [3,4].

In a Fermilab-Los Alamos collaboration experiment, inductances sufficient to cancel a large fraction of the space-charge potential well distortion were installed in the Los Alamos Proton Storage Ring (PSR). The PSR beam intensity has been limited by the onset of a transverse ep instability caused by electrons trapped in the proton beam potential well. An h = 1 rf bunching system is operated to create a gap in the proton beam to allow trapped electrons to escape. With increasing beam intensity the effectiveness of the rf system is compromised by beam induced potential well distortion, and small numbers of protons escape the rf generated potential well and drift into the gap. Initial results of the experiment indicated that the inductors increased the effectiveness of the rf bunching system such that significantly larger beam intensities could be attained [5,6].

Because of the geometry of the introduced ferrite rings and the real and imaginary properties of the ferrite permeability at high frequency, the installed inductors caused an unacceptable self-bunching (microwave-like) instability. This problem was solved by heating the ferrite in such a way that the Q and the shunt impedance of the offending resonance were reduced so that no instability occurs at the PSR design intensity. An added benefit of the heating is that the real permeability of the ferrite is increased to a level such that the installed inductors almost exactly cancel the beam-induced distortion. No additional inductance was required to reach the design intensity.

The Proton Driver design group will take advantage of the added inductance to minimize the requirement for installed rf capability in the 53 MHz Stage 1 design. It may also be useful to utilize installed inductance to enhance the performance in Stage 2 following injection capture and during bunch manipulation to create narrow bunches.

5.1.2 Direct Space Charge Compensation

As the 0.27 μC charges in each bunch (Stage 2) pass through the gap capacitance C of each rf cavity, a decelerating voltage approaching q/C may be developed, so that the charges in the bunch do not all see the same accelerating voltage. If, for instance, the effective gap capacitance were 100 pF, the voltage developed may reach 2.7 kV, a significant fraction of the design gap voltage. The developed voltage may be reduced by increasing the effective gap capacitance (effectively lowering the cavity R_s/Q). At significantly higher beam intensity (a future possibility), the effect may be countered through the addition of a second power amplifier tube with its anode connected directly to the down-stream side of the gap capacitance. This additional tube may be pulsed in a feed-forward configuration so that it delivers an electron charge to the gap capacitor approximately equal to the beam bunch charge during the bunch passage, thus minimizing the pass through charging effect of the beam.

5.1.3 Single Frequency High Gradient Burst Mode RF Cavity

Research and development for a very high gradient fixed low frequency rf cavity, (~ 600 kV per meter), is in progress here and at KEK Japan. Such a cavity could be installed to add to the rf voltage during bunch rotation for the development of narrow bunches at extraction.

5.2. Stage 1 (53 MHz) RF

5.2.1 RF Voltage, φ_s, Bucket Area, Simulations

In Phase I the Proton Driver is used with the Main Injector and possibly a neutrino factory; the defining property is a beam intensity of 3.0×10^{13} protons/pulse. In Stage 1 the Proton Driver serves only to replace the present Booster for injection into the Main Injector and possibly for low energy neutrino production. It will employ refurbished Booster rf cavities, modified to give a 5 inch aperture. The design parameters used to define the rf requirements for Phase I, Stage 1 are collected in Table 5.2.

Table 5.2. Stage 1 Proton Driver rf Parameters

E_{inj}	injection kinetic energy	400	MeV
	Beam intensity	3×10^{13}	p/cycle
	Cycle repetition	15	Hz
E_{ex}	extraction kinetic energy	12	GeV
R_{eq}	circumference/2π	113.21	m
V_{rf}	maximum rf voltage	1.2	MV
V_{acc}	accelerating voltage at dp/dt max	1.09	MV
h	harmonic number	126	
	number of populated buckets (at extraction)	119	
ε_l	longitudinal emittance at extraction	0.1	eV-s
	bunch intensity	2.5×10^{11}	
ΔE_{inj}	energy spread at injection	± 0.5	MeV
α_0	momentum compaction	-1.306×10^{-3}	
α_1	coefficient of $(\Delta p)^2$ in path length	8.252×10^{-2}	
b	vacuum chamber radius	6.35	cm
a	mean beam radius at injection	4.44	cm

The combination of performance demands with the mandated use of the 400 MeV Linac injector and modified Booster cavities calls for some unconventional measures. The specified intensity and emittance put the Proton Driver into the class of high brightness synchrotrons. The space charge impedance corresponding to the perfectly conducting wall force is $Z_{\|}/n \approx -340i\ \Omega$ at injection energy. To control the space charge defocusing, a tunable inductive insert is proposed, which will cancel this impedance throughout most of the cycle. The insert looks very attractive in the modeling; it makes the difference between 96.8 % and 99.99% for the particle transmission efficiency of the complete cycle. The idea is not new [2]; it has been tried in two different machines (Section 5.1.1). However, the studies have not been carried out over a wide range of beam energy or momentum spread and more beam studies are needed.

The next subsection gives curves for the time dependence of parameters, which change during the acceleration cycle; it is followed by a subsection with details of the

scenario, beam physics, and description of the optimization process, considerations substantially reducing the scope for arbitrary choice of the parameter curves.

5.2.1.1. Parameter Programs – Stage 1 RF Curves

The magnet ramp is driven by a 15 Hz resonant power supply plus an independent second harmonic supply that is adjusted in phase and amplitude to minimize the required peak rf voltage. The fixed parameters are those in Table 5.2. The design optimization has been carried out primarily by multi-particle tracking simulation; the results include the time curves, a demonstration of potential for low loss operation, and a demonstration that the specification for longitudinal emittance at extraction is reasonable. Because the rf voltage limit is so stringent, loss limitation naturally relates closely to longitudinal emittance preservation.

The curves in Figs. 5.1 - 5.5 present the momentum p, its time derivative dp/dt, the peak rf voltage $V_{rf,}$ the synchronous phase ϕ_s, and the h = 1 reactance of the inductive insert. In this last case, three optimum levels with optimum break times are shown. Also shown is a continuous dotted curve, calculated to just cancel the space charge force. The issues related to the optimum for this curve are examined in the following subsection.

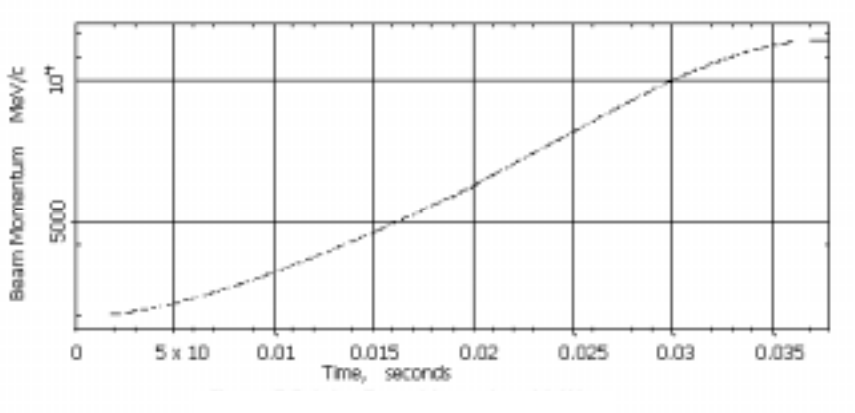

Figure 5.1. Beam Momentum, MeV/c

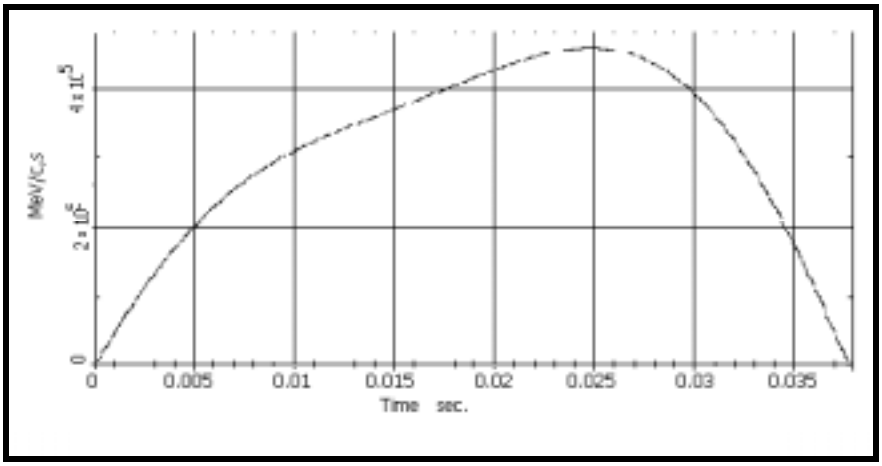

Figure 5.2. Rate of change of momentum, dp/dt vs. time, Stage 1

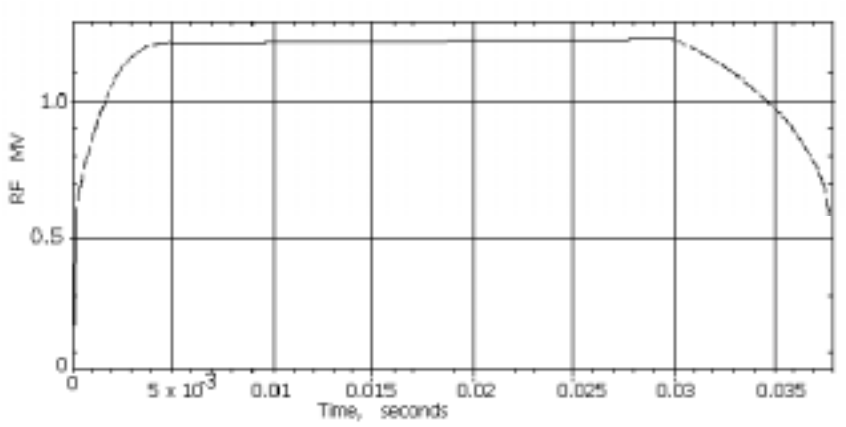

Figure 5.3. Stage 1 rf voltage in MV

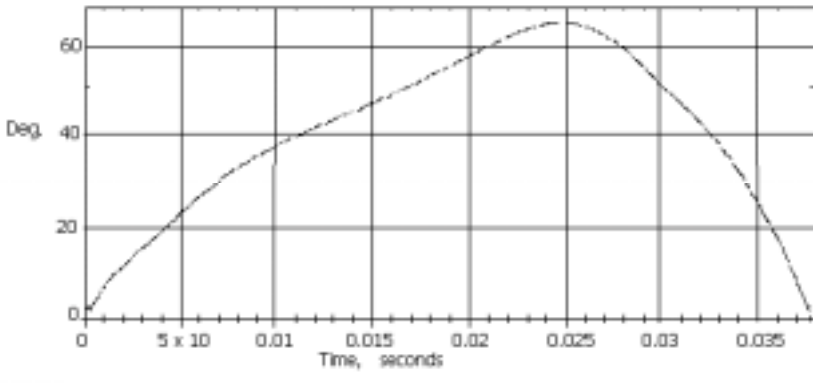

Figure 5.4. Synchronous phase angle, ϕ_s, during Stage 1 acceleration

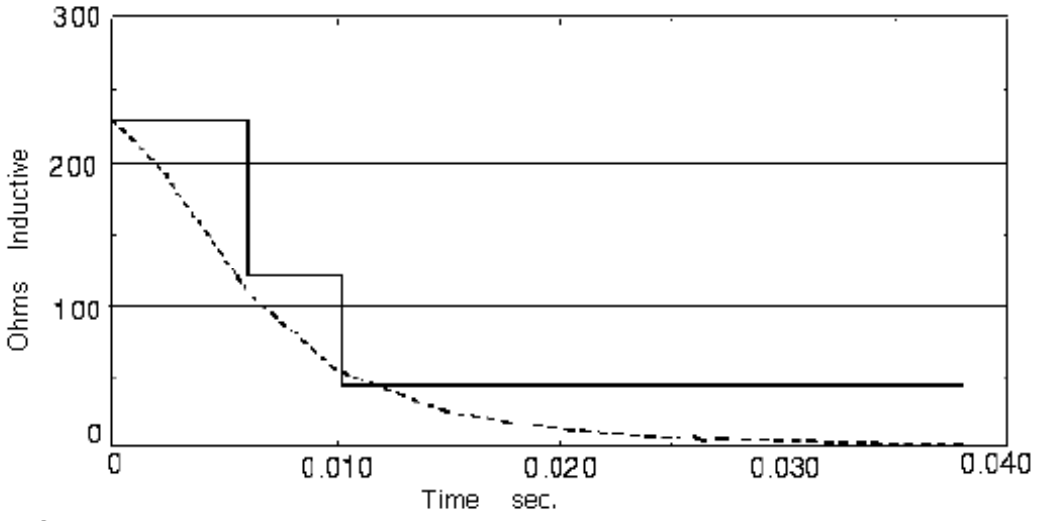

Figure 5.5. Reactance of the inserted inductor at rotation frequency (h = 1) as a function of time during acceleration

The curves in Figs. 5.6 - 5.8 present useful derived quantities, viz., synchrotron tune ν_s, bucket area S_B, and the rms longitudinal emittance per bunch ε_l.

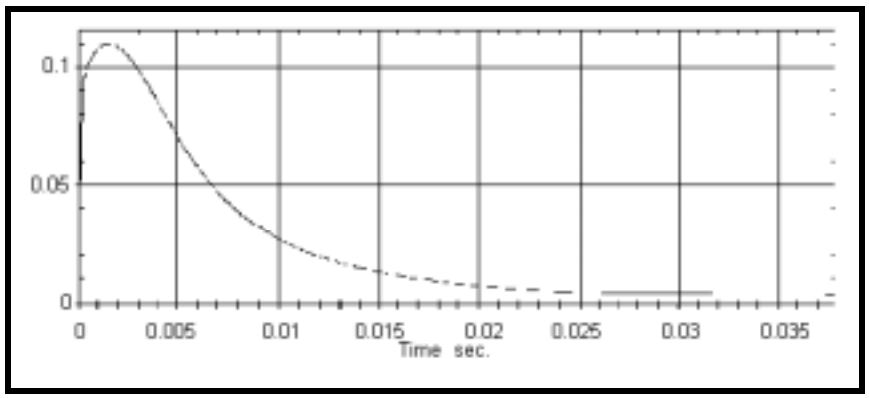

Figure 5.6. Small amplitude synchrotron tune, units of F_{rot}

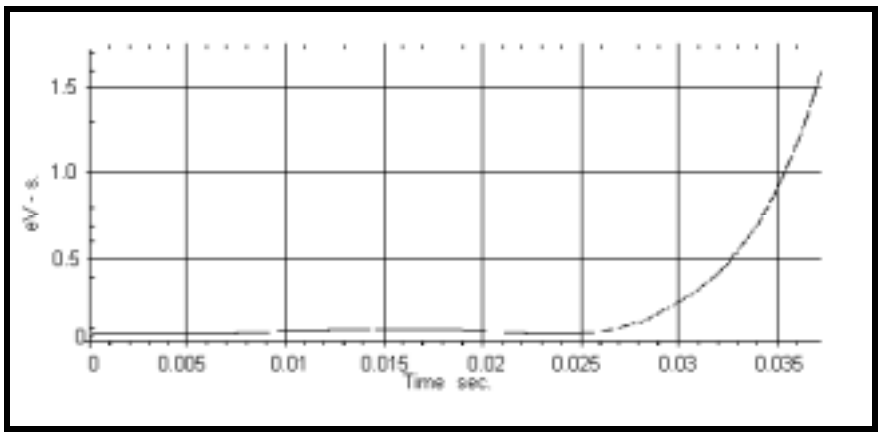

Figure 5.7. Stage 1 rf bucket area, eV-s

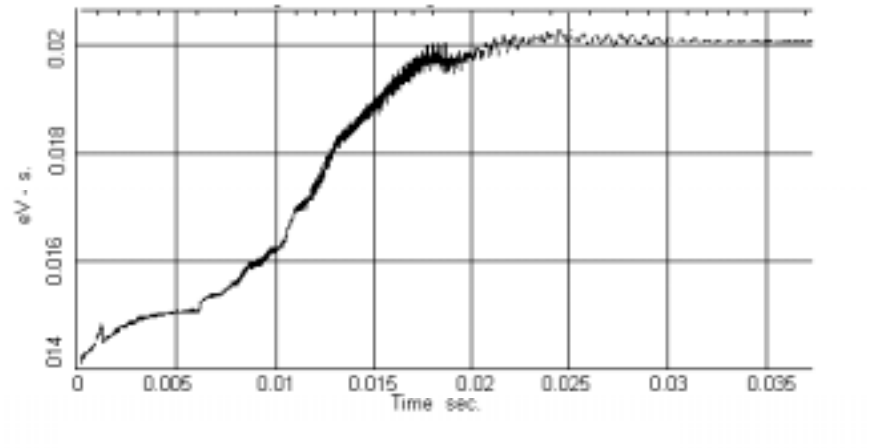

Figure 5.8. Stage 1, rms longitudinal emittance, eV-s

5.2.1.2. Capture and Acceleration – Stage 1 Scenario and Modeling

A macro-particle tracking model has been used for the entire cycle from multi-turn injection through matching to Main Injector buckets. The injected protons are assumed to be a continuous coasting beam lasting up to 90 μs, timed symmetrically about dB/dt=0. Other timings have been tried as well, but for an injection period this short nothing better has been found. For nominal Linac intensity, 70 μs is sufficient to give the required 3×10^{13} protons, but efficiency remains good over a longer injection time. A good approximation is to represent continuous injection by injections every other turn. The beam charge is raised in concert with the macro-particle injection; the perfectly conducting wall term and the inductive insert are the only sources of the collective potential included in these simulations.

The rf voltage is raised linearly during injection from 0 to 65 kV. Because of the large slip factor η for this machine, the particles near $\pm 180^{o}$ of rf phase are all captured in this simple maneuver. Certainly some are quite close to the separatrix and subject to later loss because of space charge and limited rf voltage, but these losses are essentially eliminated by use of the inductive insert. They could also be largely eliminated with a substantially higher rf voltage capability. After 226 μs, the voltage curve is changed to provide a bucket area that grows slowly to 0.064 eV-s at 4.96 ms. At this time the voltage has reached the design limit of 1.2 MV and it is held at that value until η has dropped sufficiently, at about 30 ms, to allow a reduction while continuing to increase the bucket area. dB/dt reaches zero at 37.93 ms. The voltage required for acceleration at maximum dp/dt is 1.09 MV, so there is little rf focusing. The synchronous phase reaches 64^{o}. Although dp/dt continues to increase, the magnet ramp has been tailored so that the bucket area does not decrease; in fact it rises slightly in the middle of the flat part of the voltage curve. Nonetheless, in the absence of the inductive insert there are losses at maximum dp/dt (about 0.025 s into the cycle). This indicates that the specified maximum rf voltage is marginal and the inductive insert could be very important.

There are three ways in which these modeling efforts have fed back to change somewhat the initial design ideas. One way is that the optimum magnet ramp has been determined as a minimum V_{rf} ramp rather than a minimum dB/dt ramp. Another change is the discovery of the apparent effectiveness of an inductive insert and its importance for low beam loss with h = 126 rf. Finally, it was noticed that the slip factor is so high at injection that the captured beam displays significant energy-phase correlation (bunch tilt). Precious bucket area is wasted; beam is lost because the momentum spread is increased by the tilt. Dividing the rf into 2 parts on opposite sides of the ring made a substantial improvement in the tilt and resulting loss. Dividing the rf into 3 equally spaced groups would make a small additional improvement. The planned configuration of the injection, extraction, and collimation systems may be inconsistent with the 3-way division.

Table 5.3 shows the injection-to-extraction transmission efficiency and emittance at extraction for different departures from the optimum modeling result. The top entry is the best result obtained, and each entry following gives the transmission when one condition is changed without attempting to re-optimize the other parameters. Possibly some of the

apparently lost efficiency could be recovered in such a re-optimization, but the intention is only to suggest the importance of various conditions to the optimum obtained. The lower final emittance for the more closely grouped cavities reflects directly the removal of halo by having the bunch tilted in the early part of cycle. The 95% emittance at extraction is 0.08 eV-s for the optimum case.

Table 5.3. RMS emittance at extraction and fractional beam loss during a complete cycle for optimum parameters and cases each differing from the optimum in a single property

Optimum case	0.0201 eV-s 0.01%
All rf clumped	0.0154 eV-s 0.21%
rf in two sets	0.0181 eV-s 0.07%
no inductive insert	0.0247 eV-s 3.19%

Clearly the inductive insert is a significant element in this scenario; a limited amount of rf focusing is supplemented with a self-excited focusing voltage. The character of the inductance curve suggests that there is room for refinement here. It is natural to consider tuning the inductance to just cancel the space charge impedance at all times, and indeed this could be a satisfactory mode. However, it is not a straightforward matter because a pure inductance will not cause instability even if it over-compensates, and extra focusing should be helpful. There are at least three sources of real impedance which could decelerate self-excited bunches out of the 53 MHz bunch at some higher frequency, i.e. the inductor could cause self-trapping instability. The impedances which should be taken into account at a minimum in constructing a good model are the resistive wall, the broadband beam pipe impedance from miscellaneous sources (the usual $Z_{\|}/n$), and the resistive component of inductor impedance. Permeability and loss factor curves for a Transtek Yttrium garnet ferrite have been used. The real impedance of the inductor is approximated by a 45 MHz Q = 50 resonance with R_{shunt} = 13 kΩ; $Z_{\|}/n$ = 5 Ω is included in the impedance tables that represent the inductance of the insert.

The resistive wall term is expected to be important only for the multi-bunch effects. The stability issues have not been adequately treated in the modeling, which is aimed at the problems of bucket distortion and bucket area loss. The charge distribution is smoothed to take out high frequency fluctuations, which are principally numerical noise. Once a realistic longitudinal impedance has been specified, it will be appropriate to track a portion of the cycle with enough macro-particles to represent the beam current Fourier spectrum up to 1 GHz or so.

The inductive insert is an important area for development in modeling and in machine studies as well. The Fermilab Booster is a suitable machine for investigating the effectiveness of an inductive insert, and it has also a reasonable prospect for obtaining an operational benefit.

5.2.2 Fermilab Booster Cavity Upgrade

A proposal [7,8] to modify the existing Booster rf cavity was made in January, 2000. In this proposal, two goals were set forth: (1) to enlarge the cavity beam pipe aperture from 2.25 to 5 inches; (2) to increase the cavity voltage by 20%, from 55 kV to 66 kV. The motivation for this effort is twofold. For the existing Booster, aperture enlargement will result in less activation of the rf cavities and power amplifiers, thereby permitting access to the cavities for regular maintenance during future high duty factor operation. Increased cavity voltage will allow for operation with fewer than 100% of installed cavities, thereby reducing downtime due to unscheduled maintenance. For the Proton Driver, aperture enlargement is necessary to accommodate the higher beam intensity with acceptable beam loss. The increased cavity voltage is required to increase the beam energy from 8 to 12 GeV without increasing the acceleration cycle time.

5.2.2.1. Overview of existing Booster rf cavities.

The Booster depends on 18 rf cavities for acceleration, each cavity providing approximately 55 kV over a frequency of 37 to 53 MHz. Hence, a ring voltage of 990 kV is achieved. (A voltage increase of 20% would raise the ring voltage to 1188 kV.) The rf cavity is a center-fed coaxial double-gap structure with an electrical length of 136 degrees, gap-to-gap, as illustrated in Figure 5.9. The 150 kW power amplifier is mounted directly to the cavity and is coupled to the center conductor via a 1200 pF anode dc blocking capacitor. The cavity frequency is controlled by three ferrite-loaded variable inductors attached at the center of the cavity in parallel. The ferrite bias windings are series connected and driven by a 2500 A programmable bias supply. Near the accelerating gaps at each end of the cavity are 12 inch o.d. conical coaxial alumina windows separating the beam vacuum from the air-filled center section of the cavity. The gap spacing is 0.9 inches and the beam aperture is 2.25 inches. The cavity anode to gap voltage step-up ratio varies from 1.2 to 1.6 over the tunable frequency range. Figure 5.10 is a photograph of the cavity.

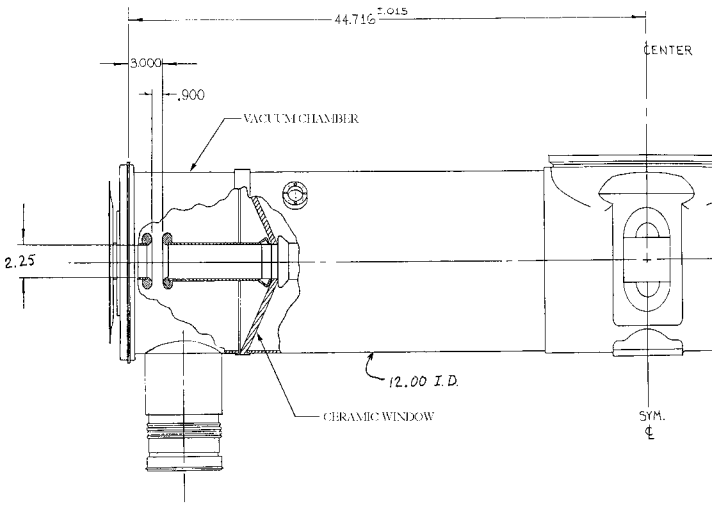

Figure 5.9. Detail of Booster cavity gap geometry

Figure 5.10. Booster cavity with ferrite tuner in foreground

5.2.2.2. Prototype large aperture Booster rf cavity; aperture enlargement and tuning.

A damaged Booster rf cavity has been the basis of the prototype work to date. Both ceramic windows, one of which was already broken, were removed to allow for extraction of the cavity center conductor. The center conductor was cut off along the taper on both sides of the center hub and new 5.5 inch outside diameter ends were attached along with variable spacing gap electrodes. The 5.5 inch diameter was chosen to allow for an inside diameter of 5 inches including the required vacuum beam tube and a high permeability cylinder intended to shield the beam from tuner magnetic fields. The end plates of the cavity were modified to match the 5 inch aperture. Gap spacing up to 3 inches can be achieved with the prototype cavity. Alumina washers were purchased to approximate the capacitive loading that will be present in a new vacuum window design.

As a first step, two standard Booster cavity ferrite tuners were mounted on the modified cavity prototype and measurements were performed with a special cut-away power amplifier that allows access to the amplifier tube anode via the screen basket. The impedance at the anode of the tube can be measured by inserting the probe of a vector voltmeter into the screen basket between the anode and screen. The ferrite tuner bias current is set and the frequency of the vector voltmeter is adjusted until a phase angle of zero, (real load), is indicated. Following this procedure, curves of anode impedance versus resonant frequency may be measured for various configurations.

Three tuner configurations were explored: two Booster tuners, three Booster tuners, and two Booster tuners with one Main Injector tuner. The resulting anode impedance versus cavity frequency is shown in Figure 5.11. For comparison, the data for a standard Booster cavity is included. Clearly the lower inductance of the Main Injector tuner is necessary to make up for the increased capacitance resulting from the cavity aperture increase. Two different gap spacings were investigated: 0.9 inch and 2 inch. As expected, the larger gap spacing results in a slightly higher upper frequency limit due to

the decrease in gap capacitance. These data do not extend to higher frequencies because the first measurements were performed using only a 1000 A bias supply.

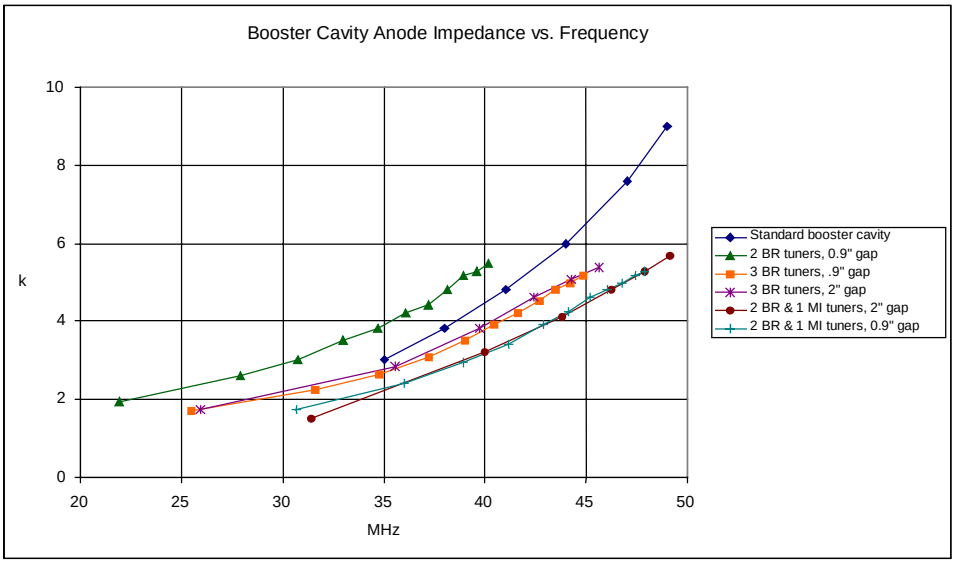

Figure 5.11. Curves of prototype cavity anode impedance versus resonant frequency for various tuner and gap configurations

Based on the foregoing results, the prototype cavity, configured with two Booster tuners and one Main Injector tuner, was moved to the MI–60 test station, where first tests with a 2500 A bias supply were recently performed. Bias currents from 0 to 2500 A provided a frequency tuning range from 29.8 to 53.4 MHz with a gap spacing of 0.9 inches. For comparison, a standard Booster cavity has a maximum frequency of 53.3 MHz. These data are shown in Figure 5.12.

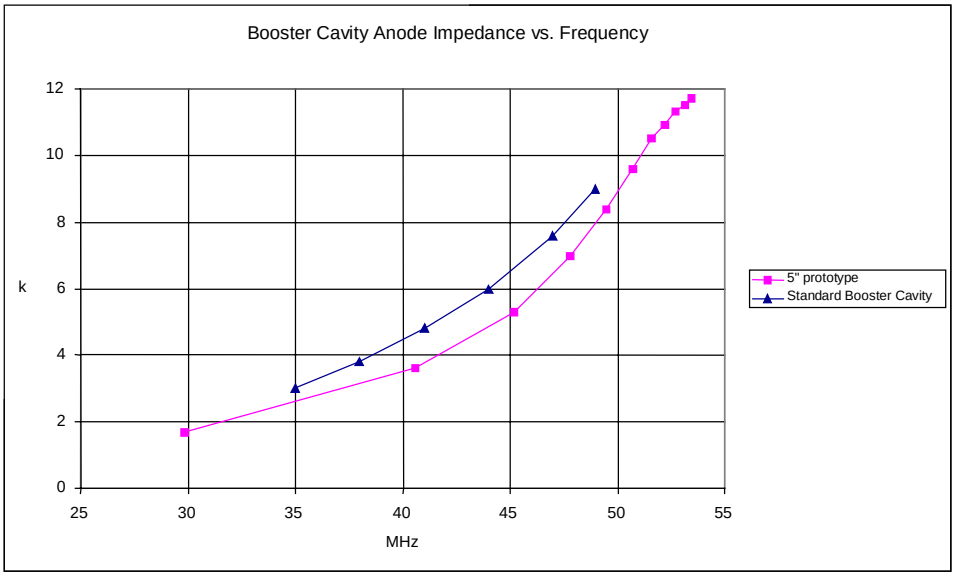

Figure 5.12. Curves of anode impedance versus resonant frequency comparing the prototype and standard Booster cavities

5.2.2.3 Cavity shunt impedance, Q, and R_s/Q

The impedance shown is the impedance presented to the power amplifier by the cavity with no beam loading. These impedances, coupled with the tube anode rf swing, can be used to calculate the dissipation in the cavity. However, they do not represent the true shunt impedance of the cavity as seen by the beam. The beam effective shunt impedance is obtained by multiplying the measured anode impedance by $4 \times S^2 \sin^2\Delta$, where S is the voltage step-up from hub to gap and Δ is the hub to gap electrical length.

The prototype R_s varies from ~ 11 kΩ to 56 kΩ between 30 and 50 MHz. The Q of the prototype cavity has recently been measured to vary from ~230 to 900 over the same frequency range. From these data it can be inferred that the effective R/Q ranges from ~50 to ~60, reaching a maximum value ~69 at 45 MHz.

5.2.2.4 Raising the Voltage

Achieving higher ring voltage might be accomplished in several ways. One technique is to simply install more cavities. There exist enough Booster cavity components to install a total of 21 modified cavities in the Proton Driver, and sufficient rf space exists in the lattice to accommodate these cavities. With 21 cavities operating at the present voltage of 55 kV per cavity, a ring voltage of 1155 kV would be obtained. This figure is not far from the 1188 kV number derived from 18 cavities operating at a 20% higher voltage (66 kV). A second way to achieve higher voltage is to raise the anode voltage on the power tubes to approximately 30 kV. This technique will be explored on the test station at MI–60 upon completion of the high power prototype cavity. A third way to higher voltage is to decrease the capacitance of the anode blocking capacitor from 1200 pF to 400 pF, thereby increasing the step up ratio of the cavity by about 20%. A low power prototype 400 pF capacitor has been fabricated and installed on a standard Booster cavity, and indeed an increased step up ratio was achieved, as shown in Figure 5.13. It is planned to modify an existing 1200 pF blocking capacitor in a way that will allow for high power testing in the future.

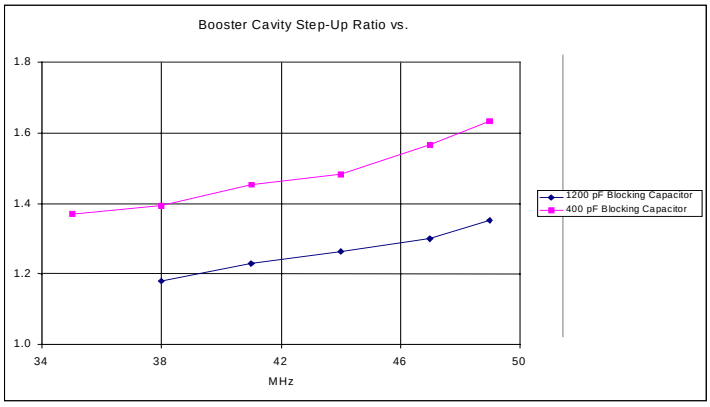

Figure 5.13 Standard Booster cavity anode-to-gap step-up ratio with 1200 pF and 400 pF blocking capacitor

One potential problem with increasing the voltage per cavity is the voltage breakdown limit of the existing ferrite tuners. The stem connection is the first place to break down when operating at high voltages. High power rf tests with the prototype cavity will confirm the maximum operating voltage as determined by this tuner limitation. This limitation might be overcome by increasing the length of the tuner stem, thereby inserting a series inductance over which some rf voltage will be dropped. This would require a somewhat different tuning inductance with which to achieve the desired frequency range of 37 to 53 MHz.

5.2.3 TRIUMF RF Cavities

An alternative to rebuilding the present Fermilab Booster rf cavities is to construct twelve new orthogonally biased rf cavities similar to the Los Alamos/SSC/TRIUMF design [9]. This type of cavity offers three clear advantages. First, higher peak accelerating voltage of 100 kV/cavity (the TRIUMF cavity has been run for several two hour intervals at 50 Hz at 62.5 kV on the gap) will require only two thirds the number of cavities in the ring. Secondly, the accelerating gradient of 94 kV/m is three times the 29 kV/m anticipated in the modified Booster cavity. This reduces the total length of the rf straight sections by a factor of three. Thirdly, the use of orthogonally biased garnets instead of the present Ni-Zn ferrites reduces the rf losses in this cavity design by at least a factor of two.

The TRIUMF prototype cavity, shown in Figure 15.14 is now at Fermilab. It has a 6 inch aperture and is tunable from 36 to 53.4 MHz. Tuning is provided by six, 60 cm OD × 30 cm ID, Trans-Tech G810 aluminum doped yttrium garnet rings. These rings are orthogonally biased by a toroidal C-magnet excited by bias current from 500 to 1050 amps. The TRIUMF cavity Q ranges from 240 to 2000 and the shunt impedance increases from 12.4 kΩ to 88 kΩ as the resonant frequency is raised. The cavity final amplifier is powered by an Eimac Y567B tetrode, identical to those used in the present Booster, Main Injector, and Tevatron rf systems.

Figure 5.14. TRIUMF Prototype Cavity

An additional six months of development work would be useful in evaluating the TRIUMF cavity. One item that needs further investigation is the cavity's

non-linear frequency response at high rf magnetic fluxes. This effect, also observed in some ferrites, is characterized by a shift in the cavity's resonant frequency to a lower frequency as the gap voltage approaches its maximum value. This frequency shifting will add an extra complication to dynamically tuning the cavity during acceleration. However, it is anticipated that a fast feedback loop around each rf station should be able to keep the cavity tuned to the correct frequency.

5.2.4 Steady State Beam Loading, Robinson Detuning.

Robinson's inequalities for maintaining longitudinal stability in the presence of beam loading are shown below. The first inequality states that the cavities must be tuned such that the fundamental frequency lies just below the resonant frequency of the cavity (below transition). The ferrite tuning loops automatically maintain this condition.

$$0 < \sin\left(2\,\Psi_z\right) < 2\,Y\cos\left(\Psi_B\right) \qquad Y := \frac{I_B}{\mathrm{Re}\left(I_T\right)}$$

The second inequality states that the cavities must deliver more power to the beam than the beam delivers to the cavity. Assuming that each cavity can deliver about 30kV to a gap with a shunt impedance of about 15 kΩ, the ratio of the beam current with respect to the in phase current of the cavity is about 1. This is still considered stable, but it is very close to becoming unstable.

The transient voltage caused by the six-bucket extraction kicker gap in the beam is less than 0.1% of the total accelerating voltage. Since transient compensation will not be necessary, only fundamental compensation is required. The same system used in the Main Injector for fundamental feedback can be modified for use in the Booster. It can provide an increase in the beam current threshold by about a factor of 14 (assuming about the same group delay from cavity drive to the gap). This will allow the RF voltage to be decreased to about 85 kV before beam loading becomes significant.

5.2.5 Stage 1 (37 - 53 MHz) RF Cavities, Power Supplies, Total Power, Water

Table 5.4 summarizes equipment and installation requirements.

Table 5.4. Equipment and installation requirements

37 - 53 MHz RF Cavities	20 Existing Booster Cavities Modified for 5 inch Aperture
High Level RF	20 High Level Booster Stations Required. Use 18 existing Ferrite Bias Supplies Use 18 existing IRM station control & data acquisition systems
New Equipment;	(20) - 200 kW Power Amplifiers. (20) - 30 kV Series Tube Modulators (20) - 6 kW Solid State Wide band Drivers. (2) - Additional Ferrite Bias Supplies (0-2500A). (2) – 35 kV Anode Power Supplies.

Existing Booster cavities will be modified to increase their aperture from 2-1/4 inch to 5 inch and gain approximately 20% in accelerating voltage over their nominal operating voltage. A large aperture prototype cavity is presently under construction. The cavity modifications are described in detail in Section 5.2.2.

Remaining components required to complete a high level station fall into two groups, one is new equipment and the other is reuse of existing equipment. Twenty rf stations are planned to meet the required 1.2 MV of peak accelerating voltage (66 kV/cavity).

A prototype 200 kW rf power amplifier is currently undergoing preliminary testing on the Booster test station at MI-60. This amplifier is a modified Main Injector amplifier with a broadband cathode drive circuit for operation over the frequency range from 37 MHz to 53.1 MHz. It utilizes the Eimac (CPI) Y567B power tetrode presently used in the Booster and Main Injector power amplifiers. This rf amplifier is grounded grid for rf but programmed dc grid bias for optimizing tube performance during the rf envelope. The amplifier will be driven by a 6 kW solid state MOSFET amplifier located in the equipment gallery.

The 6 kW wideband Solid State Driver Amplifier design is based on the Main Injector's 4 kW amplifier but with two additional 1 kW rf modules. This is a proven design with very high reliability. The 1 kW rf modules are produced by a commercial vendor.

The 30 kV Series Tube Modulator is basically a Main Injector modulator with minimal modifications. It utilizes the same Eimac (CPI) Y567B power tetrode and has a proven reliable track record. Construction drawings exist and fabrication would be straightforward.

Additional ferrite bias supplies would be exact copies of existing ferrite bias supplies presently used in the Booster. They have a proven 25-year design and are highly reliable. Construction drawings exist and fabrication would be straightforward.

Two new 35 kV 2.5 MW anode power supplies would be built. Each anode supply would supply 10 rf stations. These will be very similar to the Main Injector's anode supplies. New 13.8 kV electronic switch-gear, fused disconnect, 2 MW rectifier transformer, along with associated DC components are needed. They would be configured with an indoor DC enclosure containing the main rectifier stack, interphase reactor, capacitor bank, crowbar circuit, and high voltage disconnect switches.

Two additional IRM stations for digital I/O and analog monitoring are required. These are standard units and are widely used around the laboratory so additional units are available.

At least one and possibly two relay racks will be required per station. They will contain the station's remote controls and low level rf station control modules. Additional station control modules will have to be built since presently we are running 18 rf stations in the Booster.

To summarize, the existing equipment that will be reused consists of 18 each of ferrite bias supplies, IRM station control for digital I/O and analog monitors and control, and rf station control modules.

Overhead cable trays of standard 18 inch wide by 5 inch deep (pre-galvanized) will carry signal cables only. All rf signal cabling in trays will be HELIAX type cable. Trays will be supported approximately every 5 feet.

Since the rf system will be installed in a new building, all of the supporting utilities for the high power rf systems will be installed as part of the building construction. The LCW piping, 480/208/120 Volt AC power distribution, and cable trays will be an integral part of the construction.

Table 5.5 summarizes electrical power requirements (AC power duty factor = 50%) and Table 5.6 is a summary of cooling requirements.

Table 5.5. Summary of Electrical Power Requirements

480 Volt 3-phase		**Per station**	**20 Stations**
	Ferrite Bias Supply	105 kW	2100 kW
	Series Tube Modulator:	20 kW	400 kW
	Solid State Driver Amp	12 kW	240 kW
	RF Pump room		350 kW
120/208 volts			
	Relay racks	3 kW	60 kW
	Ion pump PS	1 kW	20 kW
	Miscellaneous	2 kW	40 kW
13.8kV			
	Anode Supply # 1		2000 kW
	Anode Supply # 2		2000 kW
Total Power			**7210 kW**

Table 5.6. Summary of LCW Cooling Requirements (duty factor = 50%)

95 Degree LCW		**Per station**	**20 Stations**
	Ferrite Bias Supply	17 gpm	340 gpm
	Series Tube Modulator:	35 gpm	700 gpm
	Solid State Driver Amp	12 gpm	240 gpm
	RF Cavity	35 gpm	700 gpm
	200 kW Power Amplifier	35 gpm	700 gpm
	Anode Supply # 1		35 gpm
	Anode Supply # 2		35 gpm
Total Flow			**2750 gpm**

The rf LCW system is a separate closed system that operates at 95 degree F with a maximum supply manifold pressure of 105 psi and a maximum return pressure of 25 psi

(ΔP = 80 psi). Conductivity must be greater than 10 MΩ cm. The heat load to the water system is approximately 5 MW.

5.2.6 Low Level RF and Global Feedback System

The purpose of the LLRF system is to develop an rf reference with the proper phase relative to the beam to maintain longitudinal stability and radial position in the presence of a varying guide field. The signals are delivered with proper phase to each rf station through a fan-out system. The LLRF system must also control the beam synchronous phase for the purpose of synchronous transfer between different accelerators and provide a beam-synchronous signal for related operations such as beam transfer, instability damping and instrumentation.

The frequency range of operation for the Proton Driver LLRF system is well within the abilities of digital signal processors (DSP) and direct digital synthesizers (DDS). A digital design makes the system very flexible. Filter parameters, gain, frequency of operation, and state machines can be modified with software parameters. This LLRF system should be able to control both the h = 126 and the h = 18 accelerators with minimal modification.

Figures 5.15 and 5.16 show the block diagrams of the phase and frequency control hardware and software.

The DSP acts as the central control processor in the system and provides the digital synthesizers with their frequency values. DDS1 provides the actual rf used to accelerate the beam. This output includes the synchronous phase angle required for acceleration. The signal is split, and each output drives half of the cavities. Each output also has its own phase shifter for counterphasing operations at injection. The DSP contains a user-defined time program that controls the values of the counterphase phase shifters.

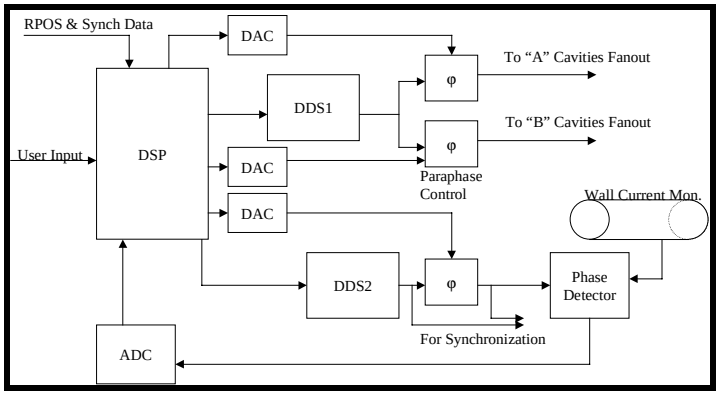

Figure 5.15. Phase and frequency control hardware

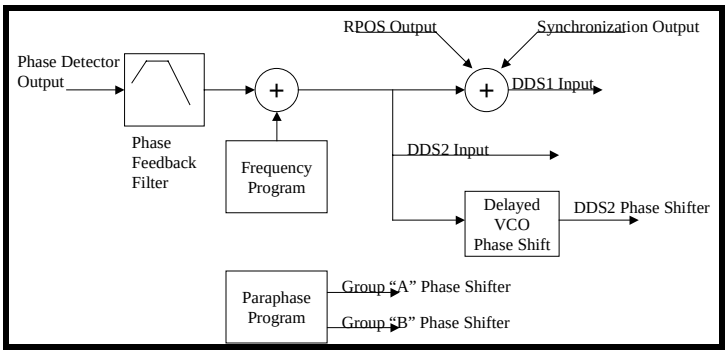

Figure 5.16. Phase and frequency control DSP function hardware and DSP function

DDS2 provides the beam synchronous rf signal. It does not contain the synchronous phase angle, so, with the proper time delay, it should always remain in quadrature with the beam signal. One of the key parameters in designing a stable LLRF feedback system is the fanout delay. The fanout delay is the time it takes for the signal from the DDS to reach each cavity gap. This delay will be about 2 μs for the Booster. It is important that the reference DDS be delayed by the exact fanout delay (plus the current monitor's cable transit time) in order to duplicate effectively the phase error as seen by the beam in the cavity. This reference delay can be generated by a long spool of cable or by an external phase shifter with a value proportional to the frequency value. The phase error is fed back into the DSP and used to adjust both the DDS1 and DDS2 frequencies to minimize the error. The DSP also contains a time table of frequency values to preempt the changing frequency and reduce phase and frequency errors.

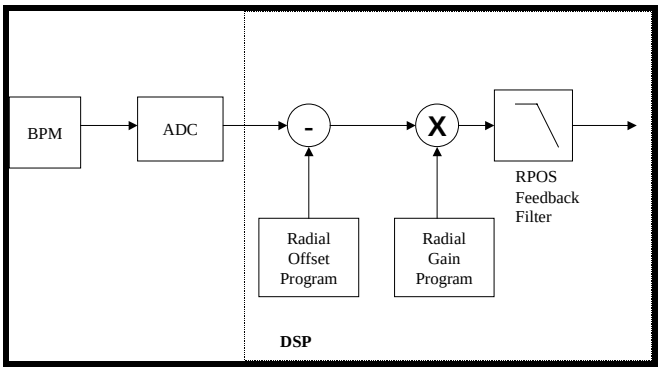

Figure 5.17. RPOS control

Figure 5.17 shows the radial position (RPOS) hardware and software functions. The position signal from a beam position monitor is sampled, and the DSP compares the value to a time-table of desired radial position values. Errors in position are filtered and summed into the DDS frequency values. The gain of the loop is controlled by another time table ramp. As the beam energy increases, the effect of frequency changes on radial position begins to increase. Also, the required bandwidth of operation begins to decrease

because of the lower synchrotron frequency. These situations make a time-varying RPOS loop gain at higher energies desirable.

Figures 5.18 and 5.19 show the block diagrams of the external synchronization control.

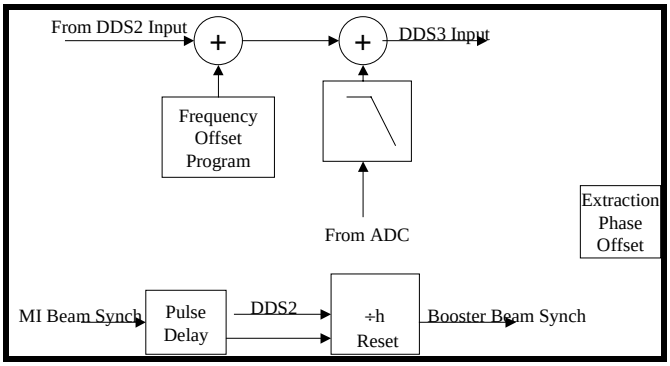

Figure 5.18. Synchronization control hardware

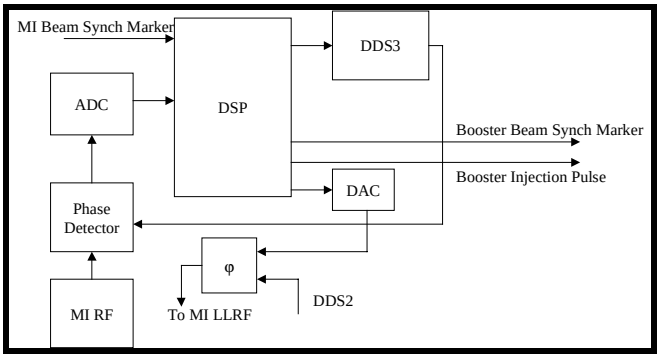

Figure 5.19. Synchronization DSP function

Maintaining phase lock to the Main Injector is the responsibility of the synchronization control. To bring the Booster beam in alignment with the proper Main Injector bucket, the synchronization control must cog the Booster beam by changing its frequency with respect to the Main Injector. The radial position of the Booster beam is not a free parameter in this process, and the RPOS loop must be disabled while attempting to phase lock to the Main Injector. The Booster lattice is designed to have a very small slip factor at extraction, which means that small changes in frequency will produce large changes in radial position. In order to keep the radial position offset to a reasonable level, phase lock to the Main Injector must start a considerable amount of time before extraction time. A 180° phase adjustment would require about 4 ms of cogging time. Cogging half the ring to line up the extraction kicker gap would require almost the entire Booster cycle.

To accommodate for the potentially long cogging periods, another DDS is used to track the Main Injector oscillator. This DDS uses the same error signal to drive its

frequency value that the beam synchronous DDS uses. The only difference between the drive of DDS3 and DDS2 is a frequency offset program that should be equal to the difference between the frequency program and the Main Injector frequency. The phase error produced by comparing this oscillator to the Main Injector oscillator is filtered and drives the fanout DDS frequency. This will produce a radial offset in the beam that will eventually bring the beam into a kind of phase lock with the Main Injector. Although the actual RPOS system is disabled during this time, it will still be possible to program a radial offset through the frequency offset program. A fixed error in this program will produce a radial offset in the beam when the synchronization loop is active. The desired radial offset can be calculated offline and loaded into the frequency offset program.

The other purpose of the synchronization control is to produce a beam synchronous pulse for generating and tracking the extraction kicker gap. Generating the pulse is quite simple; it's just a digital counter that is clocked by the rf frequency and counts up to the harmonic number. Determining when to reset the count for different injections into the Booster is rather tricky. The reset should be a function of the Main Injector beam synch marker. If a predictable relationship exists between the Main Injector markers at Booster injection and extraction, then the Booster beam synch marker could be generated by the Main Injector marker and reduce the total amount of cogging necessary to align the extraction gap. The predictability of the relationship is dependent on the accumulated RPOS error in the two machines, plus the stability of the magnetic fields. Large enough random errors in either system could eliminate the advantage to resetting the Booster beam synch marker with the Main Injector marker.

It is assumed the Main Injector will produce the extraction pulse when the phase relationship between the Booster and Main Injector rf is correct and the markers lined up appropriately. The extraction phase offset is shown as a DSP parameter controlling a phase shifter upstream of the Main Injector LLRF system. This parameter can be located and operated by the Main Injector LLRF system if necessary. The injection trigger is completely generated by the B_{min} signal from the test magnet. This signal may go through the DSP or drive the Linac chopper directly. Either way, the trigger time jitter relative to the real B_{min} must be minimized to maintain a stable magnetic field ramp for the external phase lock system to operate without large radial offsets.

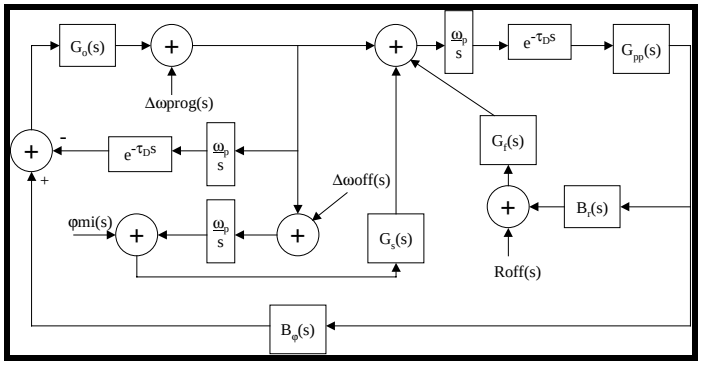

Figure 5.20. LLRF transfer functions

Figure 5.20 is the block diagram of the entire closed loop system. The transfer function equations of the phase loop and the RPOS loop are given below.

$$B_{\psi}(s) := \frac{\omega_s^2}{\omega_s^2 + .01\,s\cdot\omega_s + s^2}$$

$$B_R(s) := s\cdot B_{\psi}(s)$$

$$G_o(s) := g1\cdot\frac{\left(1 + s\cdot\tau_{dif}\right)}{\left(1 + s\cdot\tau_{o1}\right)}$$

$$G_{pp}(s) := \frac{\sigma}{s + \sigma}$$

$$G_f(s) := \frac{g_{fo}}{\left(1 + s\cdot\tau_{ri}\right)}$$

The maximum synchrotron frequency dictates the bandwidth of operation. In this case, it is about 32 kHz. This is very close to the half bandwidth of the 53 MHz cavities. An extra zero is included in the phase feedback filter in order to compensate this pole at about 40 kHz. This increases the phase margin significantly.

The transfer functions are also used to determine the errors in phase and radial position for step changes in frequency and radial position. The cascaded integrators in the RPOS loop keep the DC error at zero. The loops will still have errors for ramp inputs such as the magnetic field ramp. This ramp error can be minimized with a good frequency program. At the point of the fastest instantaneous radial offset ramp, the radial offset can be held to better than 0.1 mm by an accurate frequency program that updates at a rate close to the synchrotron frequency.

Although no detailed calculations are shown, the synchronization loop can be designed to look and operate just like the RPOS loop. It is very important, however, that the offset frequency table be very accurate (with update rates at about the synchrotron frequency) to avoid large fixed radial offsets.

5.3. Stage 2, 7.5 MHz RF System

In Stage 2 the Proton Driver is to be used to produce muons for a neutrino factory storage ring. The extraction energy is raised to 16 GeV and the rf system is replaced with an h = 18 system to provide the desired bunch spacing. A factor of four larger extracted longitudinal emittance is allowed for each of the 18 bunches compared to that for the 119 bunches of Stage 1, so the design brightness is raised by 65%. However, the larger inter-bunch gap permits chopping the Linac beam, allowing synchronous injection. The Linac beam spans 252^o of an approximately stationary bucket.

A major difference between operation as an injector for the Main Injector and Stage 2 operation is the requirement for ~ 1 ns rms bunch length at extraction. This requirement can be met by keeping the voltage at 1.4 MV even as d*B*/d*t* drops toward the end of the

acceleration cycle. Even narrower bunches can be obtained by a quarter period bunch rotation in a mismatched bucket. The momentum spread becomes wide enough that the contributions of the second and third order dependence of path length on momentum difference from the synchronous momentum are important. These contributions are included in the macro-particle model. The rms bunch length with no rotation (described above), is 1.55 ns. With bunch rotation the rms bunch length may be reduced to 0.64 ns. The final 95% emittances are 0.39 eV-s and 0.43 eV-s respectively.

The rf parameters of the Proton Driver for Stage 2 are collected in Table 5.7.

Table 5.7. Stage 2 Proton Driver rf Parameters

E_{inj}	injection kinetic energy	400	MeV
	Beam intensity	3×10^{13}	p/cycle
	Cycle repetition	15	Hz
E_{ext}	extraction kinetic energy	16	GeV
R_{eq}	circumference/2π	113.21	M
V_{rf}	maximum rf voltage	1.4	MV
V_{acc}	accelerating voltage at dp/dt max	1.33	MV
h	harmonic number	18	
	Bunch intensity	1.7×10^{12}	
	Momentum acceptance	2.5	%
ε_l	longitudinal emittance at extraction	0.4	eV-s
	rms bunch length at extraction	≤3	eV-s
ΔE_{inj}	energy spread at injection	±0.5	MeV
α_0	momentum compaction	-1.306×10^{-3}	
α_1	coefficient of $(\Delta p)^2$ in path length	8.252×10^{-2}	
α_2	coefficient of $(\Delta p)^3$ in path length	–0.4456	
b	vacuum chamber radius	6.35	cm
a	mean beam radius at injection	4.44	cm

5.3.1 Parameter Programs – Stage 2 RF Curves

The magnet ramp is driven by a 15 Hz resonant supply plus an independent second harmonic supply that is adjusted in phase and amplitude to minimize the maximum value of d*p*/d*t*. Because there is chopping and more adequate rf focusing in Stage 2, there is no need for an inductive insert. Thus, the model results given for Stage 2 require less in the way of cautionary disclaimers. With the model parameters used there is no loss during the cycle. However, the longitudinal emittance has been simulated with only the perfectly conducting wall impedance included.

The curves in Figs. 5.21 - 5.24 present the momentum *p*, its time derivative d*p*/d*t*, the peak rf voltage V_{rf}, and the synchronous phase ϕ_s when the bunch rotation is used.

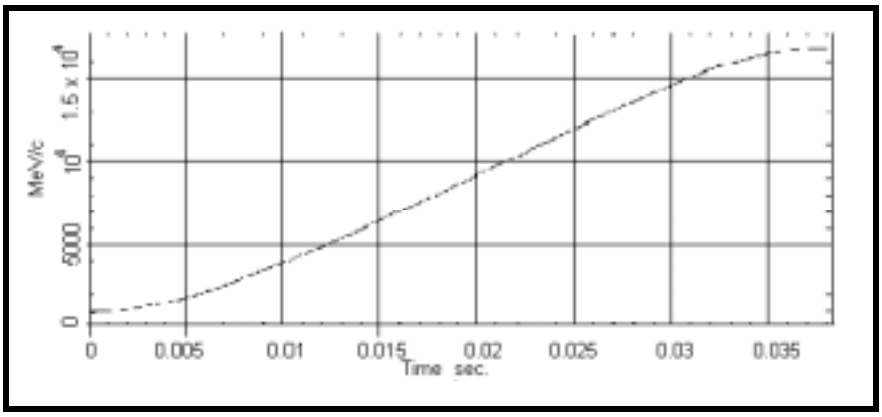

Figure 5.21. Stage 2, Beam momentum

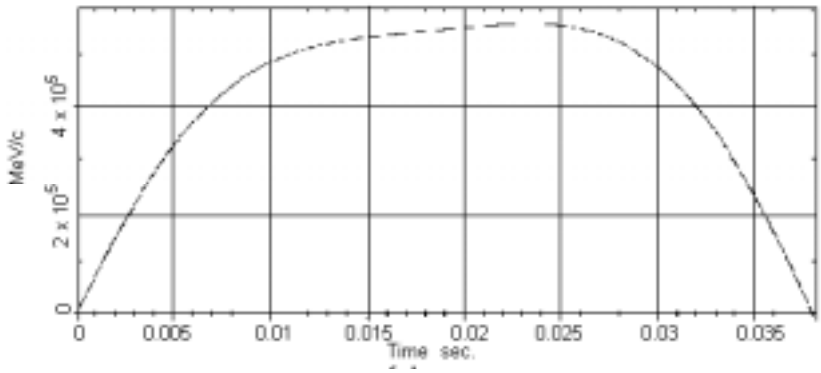

Figure 5.22. Stage 2, Rate of change of momentum, dp/dt, MeV/c/sec

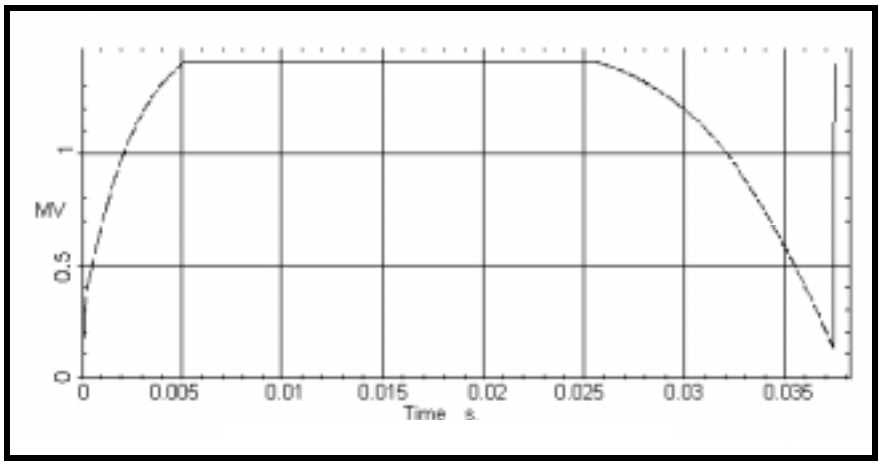

Figure 5.23. Stage 2, rf voltage

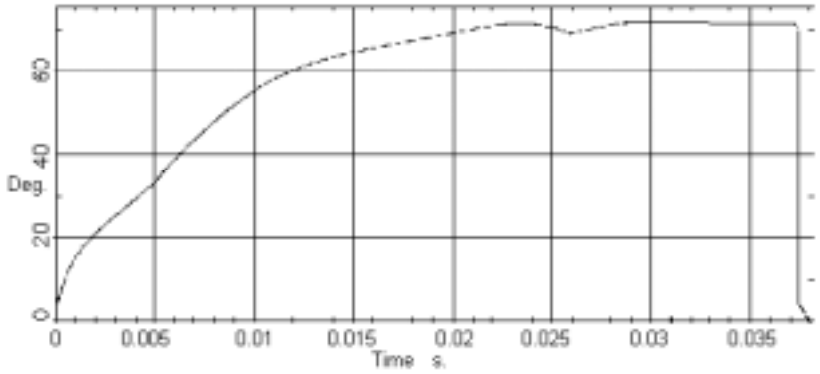

Figure 5.24. Stage 2, Synchronous phase angle ϕ_s during acceleration in degrees

The curves in Figs. 5.25 – 5.27 present useful derived quantities, *viz*., synchrotron tune ν_s, bucket area S_B, and rms longitudinal emittance per bunch ε_l. When rotation is not used, the rf voltage curve is the same through 26 ms; however it remains at 1.4 MV for the rest of the cycle.

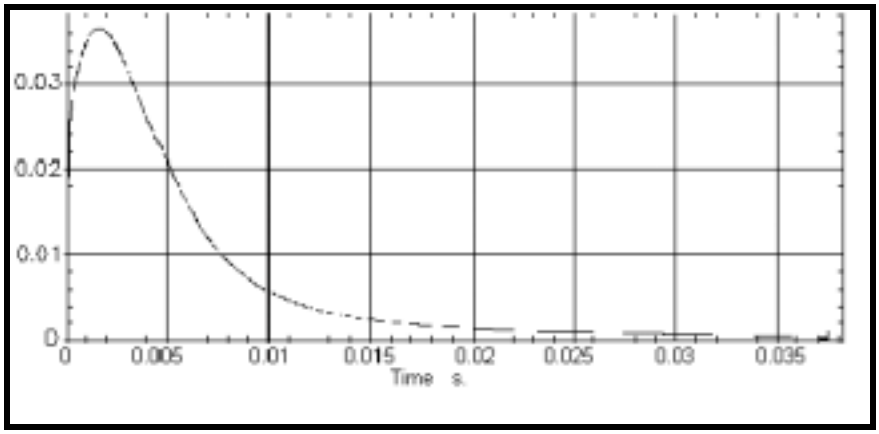

Figure 5.25. Stage 2, small amplitude synchrotron tune in units of F_{rot}

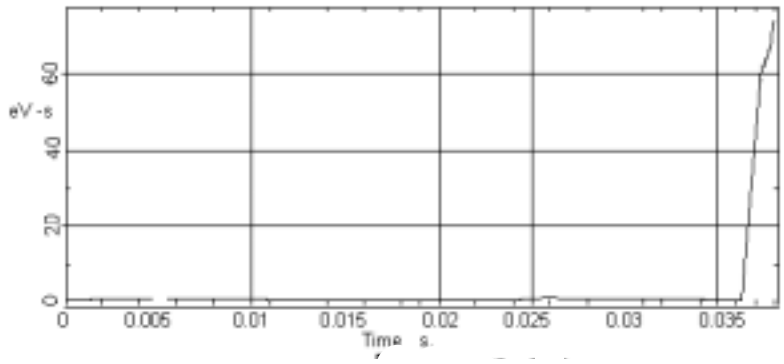

Figure 5.26. Stage 2, rf bucket area in eV-s

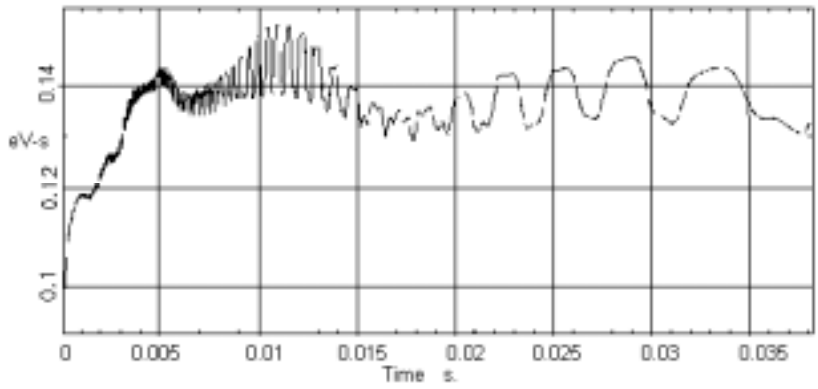

Figure 5.27. Stage 2, rms longitudinal emittance per bunch, eV-s

5.3.1.1 Capture and Acceleration – Stage 2 Scenario and Modeling

The 252^{o} chop which becomes possible with the 7.5 MHz rf system means that beam is injected into nearly stationary buckets. Therefore, losses are a much less severe problem, not only at injection, but also throughout the acceleration cycle. The voltage and magnet ramp curves are similar to those found for Stage 1, but the buckets are less full and there is no need for fine tuning of the curves to control losses.

For the narrowest bunches, mismatched bucket bunch rotation is intended. However, merely keeping the voltage at its maximum permissible 1.4 MV until the end of the cycle already gives an rms bunch length of < 2 ns, somewhat better than had been anticipated in the initial design. For injection into the Main Injector the final voltage can be set at any convenient value between 1.4 MV and ~100 kV. Fig. 5.28 shows the azimuthal projection in degrees at extraction for V_{rf} = 1.4 MV, where each degree of azimuth corresponds to 6.6 ns of bunch length. The rms length is 1.55 ns.

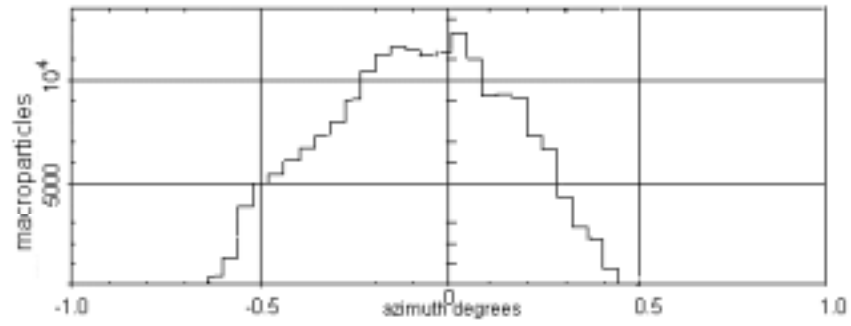

Figure 5.28. Stage 2, azimuthal charge histogram of macroparticle number in 0.02^{o} bins, at extraction without bunch rotation. Each degree represents ~ 6.6 ns.

5.3.1.2 Bunch Rotation – < 1 ns rms Bunch Length

Figure 5.29 shows the azimuthal projection of a bunch at extraction when rotated to minimum rms bunch length in a bucket produced by the maximum 1.4 MV. The rotation starts at 37.6 ms when the synchronous phase is $\phi_s = 71^o$ and V_{rf} is 124 kV. The rotated bunch has rms length 0.64 ns.

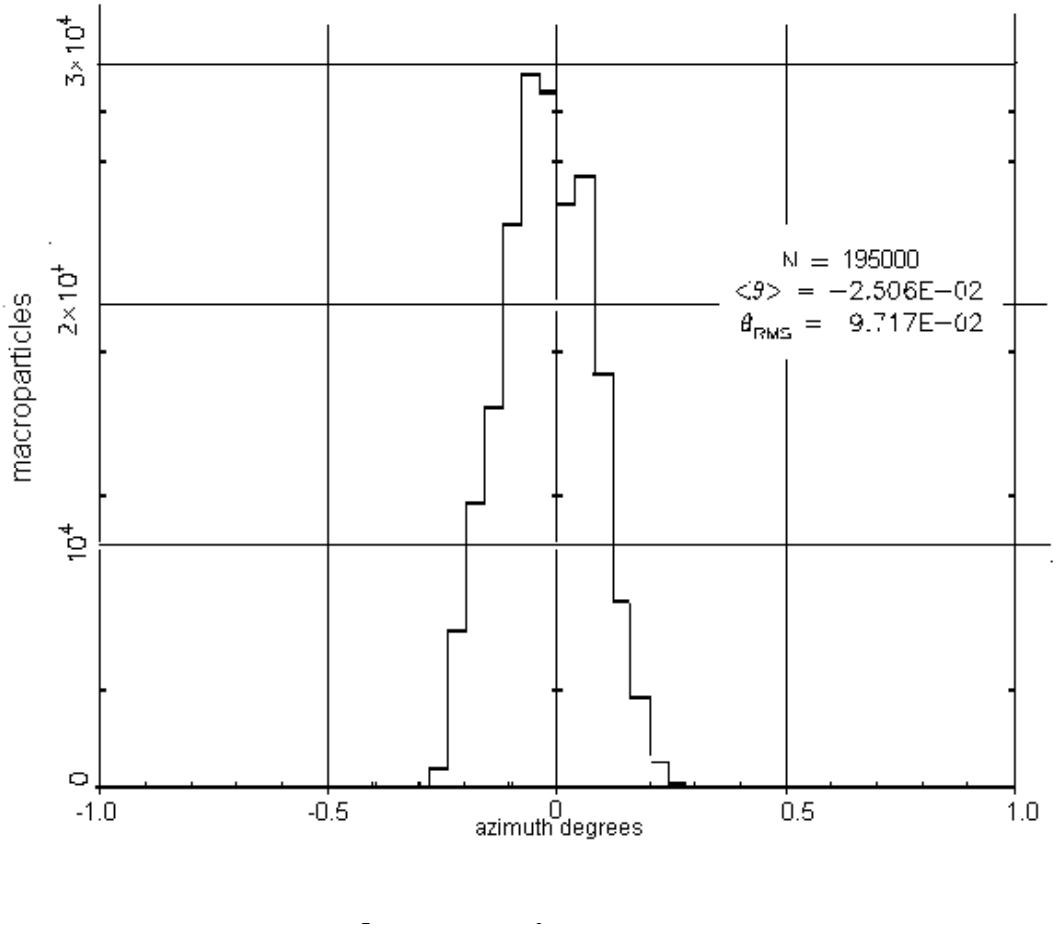

Figure 5.29. Azimuthal charge histogram of macroparticle number in 0.02^o bins at extraction with bunch rotation. One degree at h = 1 represents 6.6 ns.

5.3.2 Finemet Low Frequency rf Cavities

Stage 2 of the Proton Driver requires a large rf system operating at 15 Hz with a 60% duty cycle over the frequency range of 5.4 to 7.6 MHz. The system must be capable of producing a total peak accelerating ring voltage of 1.4 MV while delivering 3 MW of peak power to the beam. These conditions can be met with 100 rf cavities, each generating a peak accelerating voltage of 15 kV. Traditionally, rf systems operating in this frequency range have relied on nickel-zinc ferrite loaded rf cavities. However, the available tunnel space for the rf system dictates an accelerating gradient of at least 30 - 40 kV/m which is the upper limit for ferrite cavities at these frequencies.

Finemet [10], a nanocrystalline soft magnetic material, manufactured by Hitachi Metals and previously used at KEK, Japan, is a possible replacement for the nickel-zinc ferrites. Finemet has a Curie temperature of ≈ 500°C and is available in large diameter (1 meter) tape wound cores. The best available Ni-Zn ferrites can operate at a maximum rf magnetic flux, B_{rf}, between 100 and 200 Gauss. Finemet has the useful property that, unlike ferrites, it can maintain all of its normal magnetic characteristics at B_{rf} levels an order of magnitude larger (1000 - 2000 Gauss). Theoretically, this should enable an rf cavity containing Finemet cores to achieve a voltage gradient at least ten times higher than a comparable ferrite loaded cavity of the same dimensions. In practice this is probably not possible for cw operation, since the cores are very lossy at these frequencies, $Q < 1$. Under these extreme cw conditions, the Finemet cores would probably not have sufficient cooling to remain below the Curie temperature. To reduce these core losses, the Finemet cores are covered with epoxy and then cut in half to give an adjustable air gap between the two halves. Cut Finemet cores are ideally suited for use in the range of higher gradients just beyond those attainable with the Ni-Zn ferrites.

How will a Finemet cavity behave at high beam intensities under heavy beam loading? A known rf dynamics theorem is that in order to avoid Robinson type instabilities, without using rf feedback, the amount of power delivered to the beam must be equal to or less than the amount of power dissipated in the rf cavity. A lossy Finemet cavity with a shunt impedance of $R_s \approx 500\ \Omega$ provides an easy way to satisfy this stability criterion. The transient beam loading response is proportional to the ratio R_s/Q of the rf cavity. For a Finemet cavity with cut cores, R_s is relatively constant as a function of core separation while Q undergoes large changes as the core separation is adjusted. This means that once the cavity shunt impedance is fixed, the ratio R_s/Q can be lowered to suppress the transient beam loading response by simply increasing the separation between core halves to increase Q.

Early in the Proton Driver Study, it was decided to build an rf cavity using Finemet cores that could be powered by a 200 kW rf amplifier; provisions were included for adding a second power amplifier at a later date whose express purpose was to provide transient beam loading compensation. At that time in the study it was envisioned that the cavity would be used in a 3 - 16 GeV machine whose frequency sweep was only 500 kHz. For this reason the prototype cavity was designed and built to have a $Q \approx 10$ so that no dynamic tuning would be required during the acceleration cycle. During the past year, a staged approach to the construction of the Proton Driver has been developed. This led to the elimination of the original 400 MeV – 3 GeV Pre-Booster from the Stage 2 design.

Injection into the new ring at 400 MeV requires the present 5.4 - 7.6 MHz tuning range. In the next section the $Q = 10$ prototype cavity will be described, followed by two proposals on how to extend the cavity's tuning range.

As part of the US-Japan HEP collaboration, a prototype Finemet cavity has been built and tested at Fermilab. Fig.5.30 is a photograph of this Finemet cavity installed in the Main Injector tunnel.

Figure 5.30. Finemet rf cavity with attached power amplifier

The cavity is a single gap, quarter-wave coaxial structure less than 0.5 m long. It consists of five 95 cm OD × 26 cm ID × 2.54 cm thick Finemet cores cut in half and separated by 3 cm. The cores are encased in epoxy and cooled by 2.54 cm thick water-cooled copper heat sinks which are the same size as the cores (KEK is experimenting with cooling Finemet cores directly with Fluorinert FC-77). The interface between the cores and heat sinks is made using Kapton 300 CR film coated with a thermally conductive compound (Wakefield 120). The stack of cores and heat sinks is compressed together using six 1-in. fiberglass rods. The anode of the final power tetrode is capacitively coupled to the gap with a 1200 pf dc blocking capacitor. The cavity is tuned to 7.5 MHz with no additional gap capacitance. The completed cavity has $Q = 11$ and $R_s = 550\ \Omega$.

The cavity is powered by a 200 kW final amplifier which uses an Eimac Y567B tetrode. The cathode of the final tetrode is driven from the combined outputs of two Amplifier Research 3500A100 solid-state amplifiers. The prototype cavity has achieved a peak gap voltage of 17 kV for short pulses, 13.8 kV at 15 Hz with a 60 % duty cycle, and 10 kV cw. At average powers in excess of 100 kW damage has been observed after several minutes of operation on two of the corners of two of the split cores, due to the increased eddy current heating. In an attempt to alleviate this problem, rounded profiles were water-jet cut on the corners of a single core. This core has survived in the cavity without sustaining any damage. We expect that proper shaping of all of the cut core corners will eliminate this thermal heating problem and allow the cavity to achieve continuous 15 Hz operation at 15 kV with a 60% duty cycle.

Two proposals have been made as to how to obtain the required 5.4 - 7.6 MHz tuning range using a Finemet cavity. One proposal is to lower the cavity Q from 11 to 3 by decreasing the gap between the split core halves to 3 mm. Contrary to what might be

expected, lowering the cavity Q will only slightly decrease the cavity shunt impedance. However, this will increase the cavity inductance and require changing the design from a single gap cavity to a double gap cavity. The second proposal would add an external tuner (a recycled Fermilab Booster tuner) in parallel with the prototype Finemet cavity. Three of these external tuners could be run in series using one of the present Booster ferrite bias supplies. The first proposal offers the simplicity of a broadband system, but places greater demands on the power amplifier. The second proposal adds the complexity of a tuner and external bias tuning loop but gives a lower cavity R_s/Q, which will be beneficial for transient beam loading compensation. Both schemes and a combination of the two are currently under study.

5.3.3 Beam Loading and Robinson Stability

Robinson's inequalities show that fundamental beam loading is not a problem for the h = 18 system. Assuming 15 kV per cavity and $R_{sh} \sim 500\ \Omega$, the ratio between beam current and cavity current is about 0.066. This is well below the intensity criterion and will allow the total voltage to be lowered to 92 kV before fundamental beam loading becomes a factor. Transient beam loading is not a factor because all the buckets are full throughout the cycle.

One significant problem in the h = 18 system is the potential well distortion. The bunches are specified to be very narrow (1 ns) relative to the bucket size. Such a large amount of charge in a small amount of time will overwhelm the voltage gradient produced by the cavities and cause bunch spreading. One possible remedy for this problem is to install a multi-harmonic beam loading compensation system. This system would provide feedback at every rf harmonic to reduce the potential well distortion. It is important to note that for such a system to work properly the peak current delivery of the power amplifier tube must be comparable to the peak bunch current anticipated in the accelerating gap during narrow bunch passage. If the tube current capability is inadequate, the broad-band feed-back system will just drive the amplifier to saturation, resulting in inadequate compensation. A 1 ns rms bunch with total charge 0.27 μC will have peak current ~ 120 A. This is barely within the peak current capability of the Y567B tetrodes that are proposed for the system.

5.3.4 Stage 2 (5.4-7.6 MHz) Cavities, Power Supplies, LCW Water, Mains Power

In Table 5.8 are summarized equipment requirements for Stage 2. A prototype rf amplifier has been tested on the prototype Finemet cavity. This amplifier is a modified Main Injector amplifier with a broadband cathode drive circuit for operation over 5.4 MHz to 7.6 MHz. It utilizes the Eimac (CPI) Y567B power tetrode that is presently used in the Booster and Main Injector power amplifiers. This rf amplifier is grounded grid for rf but programmed dc grid bias for optimizing tube performance during the rf envelope. The amplifier will be driven by a 8 kW solid state MOSFET amplifier located in the equipment gallery.

Table 5.8. Equipment requirements for Stage 2

Finemet RF Cavities	100 cavities @ 15 kV /Cavity; prototype currently under test. One ferrite tuner per cavity may be needed (See section 5.3.2 for Cavity Details
High Level RF	100 High Level stations. If cavity tuners are required then ferrite bias supplies will be needed. 100 IRM station control & data acquisition systems
New Equipment	(100) - 200 kW Power Amplifiers. (100) - 20 kV Series Tube Modulators (100) - 8 kW Solid State Drivers. (15) - Additional bias supplies for ferrite tuners . (10) - 20 kV Anode Power Supplies.

The 8 kW wideband Solid State Driver Amplifier consists of running two commercially available 3.5 kW solid state amplifiers in parallel. An alternative would be to build a version of the Main Injector's solid state amplifier with eight 1 kW modules operating at 5.4 to 7.6 MHz.

The 20 kV Series Tube Modulator is basically a Main Injector modulator with minimal modifications. It utilizes the same Eimac (CPI) Y567B power tetrode and has a proven reliable track record. Construction drawings exist and fabrication would be straightforward. All testing of the prototype cavity and power amplifier was done with a slightly modified Main Injector modulator.

The additional ferrite bias supplies would be exact copies of existing ferrite bias supplies that are presently used in Booster. They have a proven 25-year design and are highly reliable. Construction drawings exist and fabrication would be straightforward. One supply would supply bias for multiple cavities. Depending on the final cavity design, ferrite bias supplies may not be needed.

Ten new 20 kV 2.5 MW anode power supplies would be built. Each anode supply would supply 10 rf stations. These will be very similar to the Main Injector's anode supplies. New 13.8 kV electronic switch gear, fused disconnect, 2 MW rectifier transformer, along with associated DC components are needed. They would be configured with an indoor DC enclosure containing the main rectifier stack, interphase reactor, capacitor bank, crowbar circuit, and high voltage disconnect switches.

Thirty two additional IRM station control chassis are needed. These are standard units and are widely used around the laboratory, so additional units could be purchased easily. One IRM would be required for every two stations (total 50 IRM's).

At least one and possibly two relay racks will be required per station. They will contain the station's remote controls and low level rf station control modules.

Existing equipment that will be reused are 18 each of Ferrite bias supplies, and IRM station control for digital I/O & Analog monitors and control.

Overhead cable trays of standard 18 inch wide by 5 inch deep (pre-galvanized) will carry only signal cables. All rf signal cabling in trays will be HELIAX type cable. Trays will be supported approximately every 5 feet.

Tables 5.9 and 5.10 itemize the electrical power and LCW cooling requirements. Since the rf system will be installed in a new building, all of the supporting utilities for the high power rf systems will be installed as part of the building construction. The LCW piping, 480/208/120 Volt AC power distribution, and cable trays will be an integral part of the construction. The AC power duty factor = 50%.

Table 5.9. Summary of Electrical Power Requirements

480 Volt 3-phase		**Per station**	**100 Stations**
	Ferrite Bias Supply/3 stations	35 kW	3465 kW
	Series Tube Modulator:	20 kW	2000 kW
	Solid State Driver Amp	12 kW	1200 kW
	RF Pump room		1000 kW
120/208 volts			
	Relay racks	1.5 kW	150 kW
	Ion pump PS	0.5 kW	50 kW
	Miscellaneous	1 kW	100 kW
13.8 kV			
	10 - Anode Supplies	200 kW	20,000 kW
Total Power			**27,965 kW**

Table 5.10. Summary of Cooling Requirements

95 Degree LCW		**Per station**	**100 Stations**
	Ferrite Bias Supply	17 gpm	561 gpm
	Series Tube Modulator:	35 gpm	3500 gpm
	Solid State Driver Amp	15 gpm	1500 gpm
	RF Cavity	20 gpm	2000 gpm
	200 kW Power Amplifier	35 gpm	3500 gpm
	Anode Supplies	35 gpm	350 gpm
Total Flow			**11,411 gpm**

The LCW cooling is based on a duty factor = 50%. The rf LCW system is a separate closed system that operates at 95° F with a maximum supply manifold pressure of 105 psi and a maximum return pressure of 25 psi (ΔP = 80 psi). Conductivity must be greater than 10 Ω cm. Heat load to the water system is approximately 28 MW.

5.4. R & D Plans and Proposals

5.4.1 Future Work, Booster Cavity Modification

At present the prototype cavity is installed at the MI–60 test station and is ready for high power testing. The modifications and measurements performed to date indicate the aperture enlargement goal is achievable. Upon completion of successful high power tests, the next step will be to convert the prototype cavity into a tunnel-ready model that will be high power tested at MI–60 prior to being installed in the Booster for beam tests. This step will require that all design details be addressed, including new ceramic windows, beam tubes with magnetic shielding, a rebuilt Main Injector tuner with appropriately modified inner conductors and bus bars, and myriad other details. The higher order modes of this cavity will have to be measured and compared with the existing Booster cavity. It may be necessary to develop new higher order mode couplers to damp these modes.

It is further proposed that this completed large aperture prototype become one component of a complete rf station, including a new solid state driver, power amplifier, and dc supply modulator. It is anticipated that this complete program can be completed on a two year time scale if sufficient funds and staff are made available.

5.4.2 LLRF and Beam Loading Compensation R & D

The new LLRF system should be constructed and tested on the current Booster before it is decommissioned. The current Booster already has the ability to produce an extraction kicker notch in the beam, but it does not have the ability to cog the notch for injection into a specific Main Injector bucket. Design should begin early on the new system to benefit the neutrino experiments. Tracking the extraction gap is the major non-trivial design aspect of the new Booster LLRF system. Once this is designed, built and tested, the remainder of the system construction should be straightforward.

Beam loading compensation R & D is already underway. The system that will be used for the h = 126 Booster has been commissioned in the Main Injector. Once the distributed amplifiers in the current Booster are upgraded with solid-state amplifiers, work can begin on commissioning a fundamental beam loading compensation system that will also work with the h = 126 Booster.

A multi-harmonic beam loading compensation module is also currently under construction. This module will be tested in the Main Injector for the purpose of transient beam loading compensation. The module will also be tested on the 7.5 MHz cavity that has been installed in the Main Injector. Once the cavity, power amplifiers, and beam loading modules are complete and installed, low energy and low voltage acceleration studies will be scheduled to test the systems ability to compensate the potential well distortion.

5.4.3. TRIUMF rf cavity study

In experiments at TRIUMF, SSC, and Los Alamos it has been observed that the permeability of the Yt-Garnet ferrite in the TRIUMF cavity is affected by changes in the ferrite H field due to the rf current generated by the cavity. In the Yt-Garnet case the cavity may be dynamically de-tuned by fields induced in the cavity by high beam current. It may be possible to stabilize the cavity frequency against this effect by a high gain feedback loop around the cavity. Before it is decided to augment the Proton Driver h = 126 ring voltage with TRIUMF style cavities, several months of R & D study of this problem and possible solutions would be invaluable.

5.4.4. Inductive insert study in the existing Fermilab Booster

At high beam intensity there continues to be substantial and unexplained beam loss at injection and during early phase of acceleration. There is reason to expect that introduction of space charge compensating inductors may be helpful in alleviating this loss. A detailed study of the properties of available ferrite over a frequency range spanning perhaps five Booster rf harmonics would lend strength to the argument for the usefulness of such an installation. Continued ESME simulation studies should proceed in concert with and using results of the ferrite properties study. The results of such a study may contribute to the understanding of the use of inductive compensation in a ramping synchrotron, as well as contributing to improved operation of the existing Booster.

References

[1] S. Hansen et al, "Effects of Space Charge and Reactive Wall Impedance on Bunched Beams," IEEE Trans. Nucl. Sci., NS-22 No.3, (1975).

[2] A.M. Sessler and V.G. Vaccaro, "Passive Compensation of Longitudinal Space Charge Effects in Circular Accelerators - The Helical Insert," CERN 68-1, ISR Div. (1968).

[3] K. Koba et al, "Longitudinal Tuner Using High Permeability Material," R.S.I. 70-7, (1999).

[4] K. Koba, "Longitudinal Tuner Using a New Material, Finemet," AIP Conf. Proc. 496, (1999).

[5] M.A. Plum et al, "Experimental Study of Passive Compensation of Space Charge at the LANL Proton Storage Ring," Physical Review Special Topics - Accelerators and Beams, Vol.2, 064201 (1999).

[6] J.E. Griffin et al, same title as in [5], Fermilab FN-661 (1997).

[7] W. Chou et al, "A Joint Proposal for Booster Cavity Modification," Fermilab, Jan. 12, 2000.

[8] J. E. Griffin, "Proposal to Rebuild Damaged Booster RF Cavity with Significant improvement in Aperture, Gap Voltage, and Power Delivery Capability," Draft, Nov. 1999.

[9] R.L. Poirier, "Perpendicular Biased ferrite-Tuned Cavities", Proc. 1993 PAC, 753, (1993).

[10] http://www.hitachi-metals.hbi.ne.jp/topics/prod/npo3.htm.